Human Molecular Genetics, 2008, Vol. 17, No. 11 ***1527–1539***
doi:10.1093/hmg/ddn041
Advance Access published on February 11, 2008

The intracellular accumulation of polymeric neuroserpin explains the severity of the dementia FENIB

Elena Miranda[1,*], Ian MacLeod[1], Mark J. Davies[1], Juan Pérez[1,2], Karin Römisch[3], Damian C. Crowther[1,4] and David A. Lomas[1]

[1]Department of Medicine, University of Cambridge, Cambridge Institute for Medical Research, Wellcome Trust/MRC Building, Hills Road, Cambridge CB2 0XY, UK, [2]Departamento de Biología Celular, Genética y Fisiología, Universidad de Málaga, Facultad de Ciencias, Campus de Teatinos, Málaga 29071, España, [3]Center for Integrative Biology, University of Trento, via delle Regole, 101, 38100 Mattarello (Trento), Italy and [4]Department of Genetics, University of Cambridge, Downing Street, Cambridge CB2 3EH, UK

Received December 17, 2007; Revised and Accepted February 7, 2008

Familial encephalopathy with neuroserpin inclusion bodies (FENIB) is an autosomal dominant dementia that is characterized by the retention of polymers of neuroserpin as inclusions within the endoplasmic reticulum (ER) of neurons. We have developed monoclonal antibodies that detect polymerized neuroserpin and have used COS-7 cells, stably transfected PC12 cell lines and transgenic *Drosophila melanogaster* to characterize the cellular handling of all four mutant forms of neuroserpin that cause FENIB. We show a direct correlation between the severity of the disease-causing mutation and the accumulation of neuroserpin polymers in cell and fly models of the disease. Moreover, mutant neuroserpin causes locomotor deficits in the fly allowing us to demonstrate a direct link between polymer accumulation and neuronal toxicity.

INTRODUCTION

Conformational diseases are a group of disorders caused by aberrant intermolecular interactions, aggregation and deposition of proteins (1). These diseases are typified by members of the serine proteinase inhibitor (serpin) superfamily in which point mutations result in the accumulation of polymerized proteins during their biosynthesis within the cell (2,3). The structural basis for serpin polymerization has been elucidated and shown to result from the sequential linkage between the reactive centre loop of one molecule and β-sheet A of another (4–9). The retention of polymerized serpins within a cell can cause disease through a 'toxic gain of function' while the lack of secretion of these important proteinase inhibitors causes the uncontrolled activation of proteolytic cascades and hence disease through a 'loss of function'. Mutations in the serpins have been implicated in diseases as diverse as liver cirrhosis, emphysema, thrombosis, angio-oedema and dementia (10,11). In view of the common mechanism, we have grouped the conditions that result from serpin polymerization as a new class of disease that we have termed as serpinopathies (2,10).

FENIB is a serpinopathy that presents as an autosomal dominant dementia (12–14). This disease is characterized histologically by inclusions of mutant neuroserpin within the endoplasmic reticulum (ER) of cortical and subcortical neurons. Wild-type neuroserpin is secreted from the axonal growth cones of the central and peripheral nervous system and inhibits tissue plasminogen activator (15–19). It has been implicated in regulation of axonal growth, reduction of seizure activity, limitation of damage during cerebral infarction and control of emotional behaviour and memory (20,21). Neuroserpin is found in dense-core secretory vesicles typical of the regulated secretory pathway in cells of the pituitary and adrenal glands (22), in a pheochromocytoma (PC12) cell line that over-expresses neuroserpin (23) and in primary neuronal cultures (24). Recently, a signal peptide for regulated secretion has been identified in the C-terminus of the protein and shown to be functional in anterior pituitary cells (AtT-20 cells) (24).

*To whom correspondence should be addressed. Tel: +44 1223336825; Fax: +44 1223336827; Email: em285@cam.ac.uk

We have described four different mutations in neuroserpin that cause the dementia FENIB. All four mutations affect the stability of the shutter region of neuroserpin and show a striking correlation between the predicted molecular instability and the number of neuroserpin inclusions and an inverse correlation with the age of onset of dementia (14). Two of these mutants, S49P and S52R neuroserpin, have been characterized in detail (18,25,26). We have shown that recombinant purified S49P and S52R neuroserpin form polymers at 37°C, and that S52R polymerizes 15 times faster than S49P neuroserpin. Moreover, both mutations cause the retention of neuroserpin as ordered polymers within the ER of COS-7 cells (27) and give rise to intracellular inclusion bodies in the brains of transgenic mice (28). The S52R neuroserpin mutation causes more accumulation in both models in keeping with the more severe clinical phenotype. There is no data on the cellular handling of H338R and G392E neuroserpin which are associated with the most severe forms of the disease (14).

We report here on the cellular processing of all four mutants of neuroserpin that cause the dementia FENIB. We have characterized the handling of the mutant proteins in COS-7 cells, in stably transfected PC12 cell lines and in transgenic *Drosophila melanogaster*. We have also developed a conformer-specific monoclonal antibody that detects polymerized neuroserpin and have used it to show that the intracellular accumulation of neuroserpin polymers, in both tissue culture cells and neurons of flies, correlates with the degree of instability of the mutant protein predicted by molecular modelling. Moreover, we show that mutant neuroserpin causes locomotor deficits in the fly, allowing us to demonstrate a direct link between polymer accumulation and neuronal toxicity.

RESULTS

H338R and G392E neuroserpin accumulate as polymers within the endoplasmic reticulum of COS-7 cells

COS-7 cells were transfected with wild-type, H338R or G392E neuroserpin and co-stained for neuroserpin and resident proteins of the secretory pathway (Fig. 1A). Wild-type neuroserpin was distributed in a reticular pattern that co-localized with calreticulin within the ER (top left panel) as reported previously (27) and as expected for a secreted glycoprotein. Both H338R and G392E neuroserpin (middle and right panels) formed the characteristic punctate inclusions that we have described for other mutants of neuroserpin that cause FENIB (27). These inclusions co-localized with calreticulin (top middle and right panels) indicating that they were contained within the ER. Co-staining with the GM130 Golgi marker showed that a fraction of the wild-type protein (bottom left panel) but none of the mutant protein (bottom middle and right panels) trafficked through this organelle.

The intracellular localization of wild-type and mutant neuroserpin was confirmed by digestion of proteins labelled with ^{35}S-methionine and -cysteine with endoglycosidase H (Fig. 1B). There was almost no detectable wild-type neuroserpin in the cell lysates after a 6 h chase (Fig. 1B, wild type, lanes C). However, there was an intracellular band of 50 kDa in cells transfected with both mutants of neuroserpin

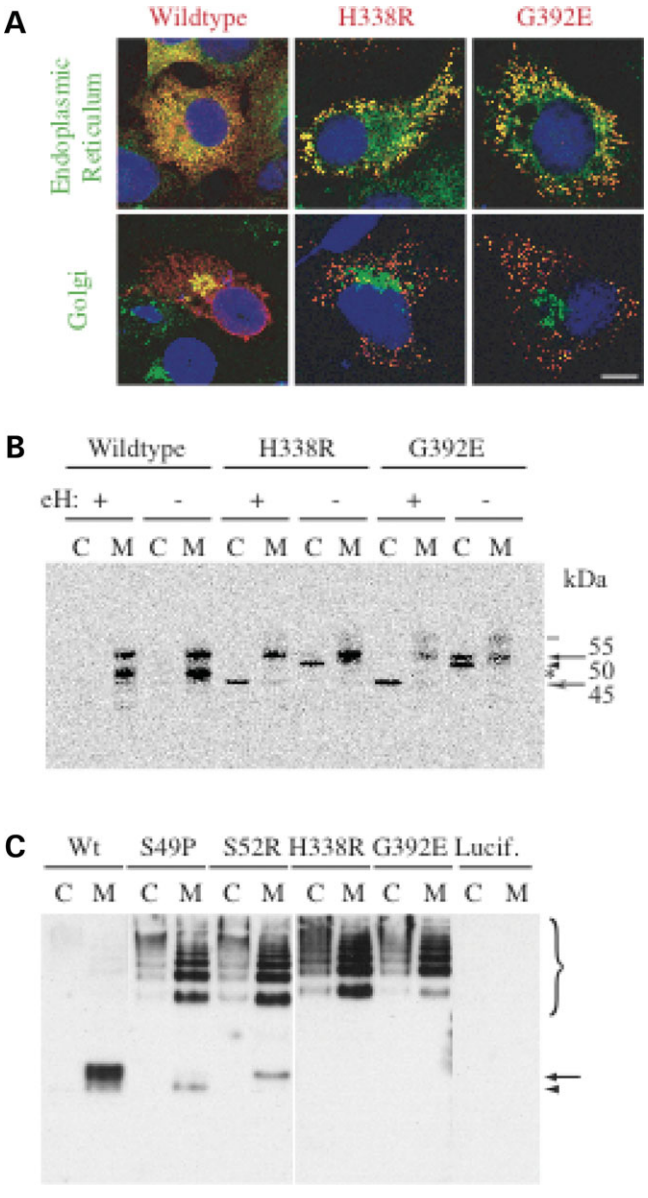

Figure 1. Mutant H338R and G392E neuroserpin accumulate as polymers within the ER. (**A**) Confocal microscopy analysis of COS-7 cells cultured for 48 h after transfection with wild-type, H338R or G392E neuroserpin and stained for neuroserpin (red) and the ER-resident protein calreticulin or the Golgi-resident protein GM130 (green). Only the merged images are shown in which yellow colour corresponds to areas with overlapping red and green staining. The nucleus appears blue due to DNA staining with DAPI. Scale bar: 10 μm. (**B**) Endoglycosidase-H (eH) digestion of samples from cells transfected with wild-type or each mutant neuroserpin that were pulsed-labelled and chased for 6 h. Cells lysates (C) and culture media (M) were analysed by immunoprecipitation and 8% w/v SDS–PAGE. Arrow: fully glycosylated and secreted neuroserpin, 55 kDa; arrowhead: intracellular neuroserpin intermediate, 50 kDa; black and white arrow: deglycosylated intracellular neuroserpin, 45 kDa; the asterisk indicates a second band of extracellular wild-type neuroserpin due to extracellular proteolysis; the dash indicates a slower migrating band of extracellular G392E neuroserpin. (**C**) 7.5% w/v acrylamide non-denaturing PAGE and western-blot analysis for neuroserpin in cell lysates (C) and culture media (M) from COS-7 cells transfected with wild-type or mutant neuroserpin or with a control plasmid expressing luciferase (Lucif.). Cells were cultured for 72 h after transfection. Arrow: wild-type and S52R neuroserpin monomers; arrowhead: S49P neuroserpin monomer; curly bracket: neuroserpin polymers.

(Fig. 1B, H338R and G392E, lanes −/C, arrowhead) that shifted to 45 kDa after digestion with endoglycosidase H (Fig. 1B, H338R and G392E, lanes +/C, black and white arrow), showing that it still contained unmodified polymannose N-glycans typical of ER proteins. None of the neuroserpin proteins in the culture media (Fig. 1B, lanes M, black arrow, 55 kDa) were sensitive to the endoglycosidase H digestion, as expected for proteins that have acquired complex oligosaccharide structures in the Golgi complex. Wild-type neuroserpin in the culture media contained an additional lower band (Fig. 1B, wild type, lanes M, asterisk) due to proteolysis over the 6 h chase period, while both mutant forms of neuroserpin were resistant to proteolysis due to their polymeric conformation (Fig. 1C). An additional band of higher molecular mass was seen for G392E neuroserpin, both within the cells (Fig. 1B, G392E, lane −/C) and in the culture media (Fig. 1B, G392E, lanes +/M and −/M, dash). Both intracellular species reduced to 45 kDa after the treatment with endoglycosidase H, suggesting that they correspond to proteins contained within the ER and that the difference between them is due to N-glycan modification.

It has been predicted that the H338R and G392E mutations cause neuroserpin to form polymers (14). This was investigated by transfecting COS-7 cells with wild-type or mutant neuroserpin and assessing the cell lysates and culture media by non-denaturing PAGE and western-blot analysis (Fig. 1C). The previously characterized S49P and S52R mutants of neuroserpin (27) were included for comparison. Wild-type neuroserpin was present solely as a monomer in the culture medium (arrow), whereas all the neuroserpin mutants formed polymers that were found in both the cell lysates and the culture media (curly bracket). In contrast to S49P and S52R neuroserpin (arrow and arrowhead in Fig. 1B), no monomeric H338R or G392E neuroserpin was detectable in the media. Moreover, G392E neuroserpin formed the highest molecular mass polymers in keeping with the prediction that it has the greatest propensity to polymerize.

Taken together, these results show that both H338R and G392E neuroserpin form polymers that accumulate within the ER.

Detection of polymers of mutant neuroserpin with an anti-polymer monoclonal antibody

We developed four conformation specific anti-neuroserpin monoclonal antibodies in order to characterize neuroserpin in our model systems of disease. We used a sandwich ELISA to determine the affinities of the monoclonal antibodies for recombinant monomeric wild-type neuroserpin and monomeric and polymeric S49P neuroserpin. The monoclonal antibodies 1A10, 10B8 and 10G12 showed similar characteristics, so we present the results for 1A10 only. This monoclonal antibody detected all three antigens with similar high affinities (Fig. 2A, top), whereas the 7C6 monoclonal antibody showed higher affinity for polymerized S49P neuroserpin (Fig. 2A, bottom). Similar results were obtained using recombinant monomeric and polymeric S52R neuroserpin as the antigen (data not shown). The monoclonal antibodies were then assessed for their ability to detect total or polymerized neuroserpin in a sandwich ELISA with different ratios of recombinant wild-type neuroserpin monomer and S52R neuroserpin polymers as antigens. 1A10 showed a similar affinity for all antigen mixtures (Fig. 2B, top), while 7C6 showed comparatively low affinity for the wild-type monomer but increasing affinity with increasing proportion of S52R polymers (Fig. 2B, bottom). We then used these monoclonal antibodies in a sandwich ELISA assay to assess the presence of neuroserpin monomers and polymers in COS-7 cells transfected with wild-type or mutant neuroserpin. The monoclonal antibody 1A10 detected neuroserpin in all the cell lysates (Fig. 2C, top) with higher signals in the lysates from cells expressing mutant neuroserpin. In contrast, 7C6 gave a clear signal in the lysates from cells expressing mutant neuroserpin but failed to detect neuroserpin in cells expressing wild-type monomeric protein (Fig. 2C, bottom). Similar results were obtained when the culture media was analysed with the same technique (results not shown). These results demonstrate the ability of 7C6 to specifically detect polymerized neuroserpin and confirm its presence in lysates and culture media of cells expressing the mutant proteins.

We then used the 7C6 monoclonal antibody to localize neuroserpin polymers in cell models of disease. Total neuroserpin was detected with a polyclonal antibody in COS-7 cells transfected with wild-type neuroserpin or one of each of the four mutants of neuroserpin that cause FENIB (Fig. 2D, red staining). In contrast, only cells expressing mutant neuroserpin showed staining with the 7C6 antibody (Fig. 2D, green staining). Cells stained in the same way with the anti-neuroserpin polyclonal antibody and the monoclonal antibody 1A10 showed overlapping red and green staining for all neuroserpin variants (data not shown). These data show that intracellular polymers contribute to the punctate accumulations of mutant neuroserpin in cell models of FENIB [(27) and the present work], and together with our ELISA results shown above demonstrate that our monoclonal antibodies are a valuable tool for the detection and quantitation of total and polymerized neuroserpin.

Accumulation of neuroserpin polymers correlates with increasing severity of dementia in patients with FENIB

The generation of the H338R and G392E mutants of neuroserpin allowed us to assess the relationship between genotype and phenotype for all four known mutations that cause FENIB. We found a striking correlation between the number of COS-7 cells that contained neuroserpin inclusions and the severity of FENIB caused by each mutation (Fig. 3A, correlation coefficient $R^2 = 0.93$). Next, we assessed the secretion of each neuroserpin variant (Fig. 3B). Neuroserpin was detected as a 50 kDa band in the cell lysates and as a 55 kDa band in the culture media, corresponding to partial and full processing of the glycan chains, respectively (Fig. 3B). After 72 h in culture, no detectable wild-type neuroserpin remained inside the cells and a strong 55 kDa band was detected in the culture medium, together with a faster migrating band due to proteolysis (Fig. 3B, Wt, lane C versus lane M). In contrast, at the same time point, we still detected intracellular mutant neuroserpin (Fig. 3B, S49P, S52R, H338R and G392E, lanes C), with the amount of neuroserpin in the cell lysates correlating with the intracellular accumulation observed by

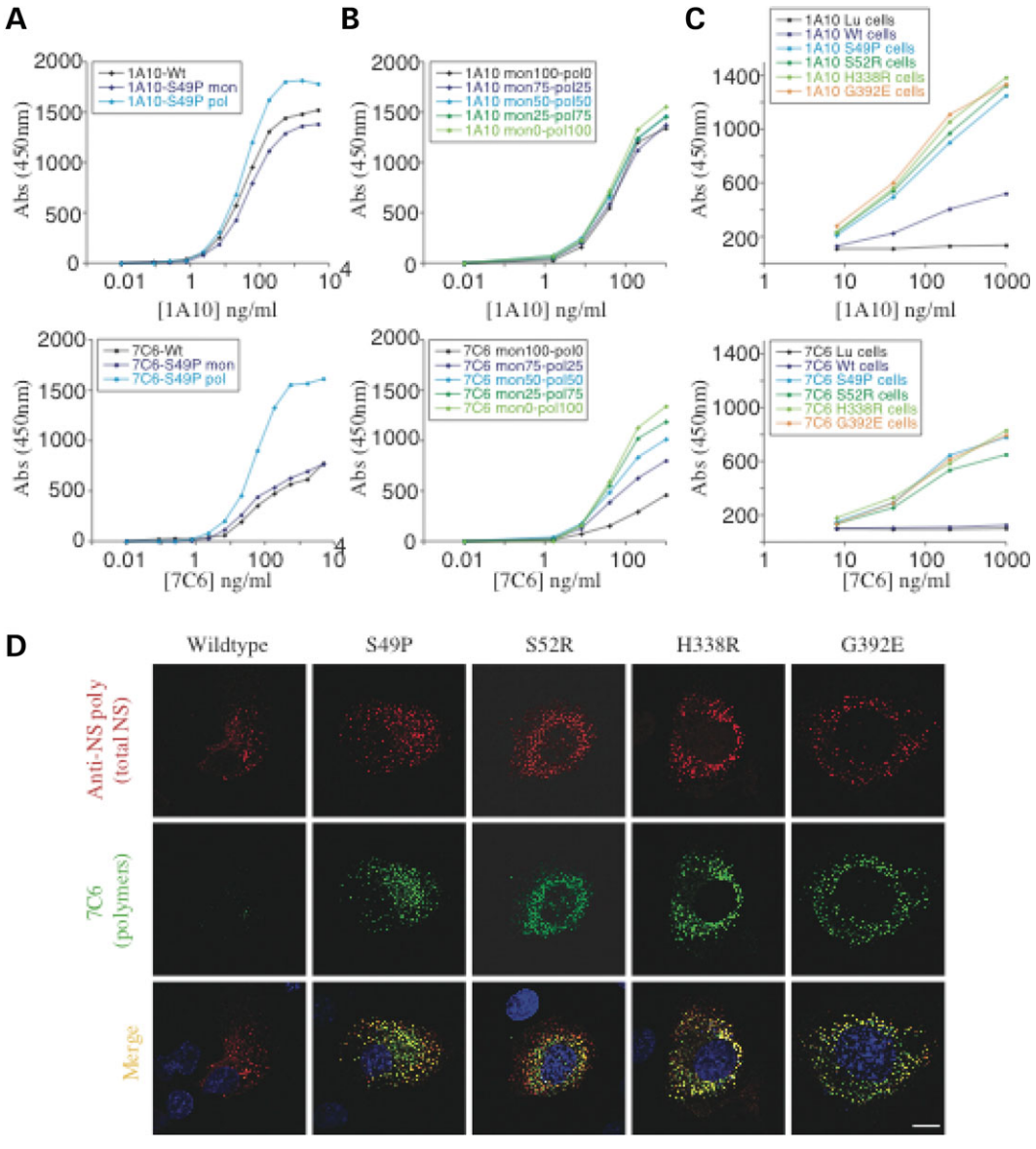

Figure 2. Detection of mutant neuroserpin polymers with an anti-polymer monoclonal antibody. (**A**) Binding of monoclonal antibodies 1A10 and 7C6 in a sandwich ELISA to recombinant monomeric wild-type neuroserpin (Wt) and monomeric (mon) or polymerized (pol) S49P neuroserpin as the antigens. (**B**) Binding of monoclonal antibodies 1A10 and 7C6 in a sandwich ELISA using different proportions of recombinant wild-type monomeric neuroserpin (mon) and polymerized S52R neuroserpin (pol) as the antigens. These are shown as the percentage of each species, for example mon75-pol25 is a mixture that is 75% monomer and 25% polymer. (**C**) Cell lysates from COS-7 cells transfected with wild-type neuroserpin or mutants of neuroserpin that cause FENIB (S49P, S52R, H338R, G392E) were analysed by sandwich ELISA using either 1A10 or 7C6 to detect neuroserpin. (**D**) Confocal microscopy analysis of COS-7 cells transiently transfected with each neuroserpin variant were immunostained for total neuroserpin with a rabbit anti-neuroserpin polyclonal antibody (red) and for neuroserpin polymers with monoclonal antibody 7C6 (green). The nucleus appears blue due to DNA staining with DAPI. Scale bar: 10 μm.

immunocytochemistry (Fig. 3A). The converse relationship was found for secretion when assessed by western-blot analysis (Fig. 3B) and quantified by sandwich ELISA (Fig. 3C, correlation coefficient $R^2 = 0.82$).

Pulse-chase analysis was used to quantify the differences in secretion between wild-type and the four mutants of neuroserpin. COS-7 cells transfected with each protein variant were pulse-labelled with ^{35}S-methionine and -cysteine for 15 min and chased for 6 h. Neuroserpin was detected as a 50 kDa intracellular band corresponding to the ER form (Fig. 3D, lanes C, arrowhead) and a 55 kDa band in the culture media corresponding to mature secreted neuroserpin with fully processed glycans (Fig. 3D, lanes M, arrow). The intracellular fraction of G392E neuroserpin also contained a 55 kDa band (Fig. 3D, lower panel, G392E, lane C) and a slower migrating band was detected in the culture medium (Fig. 3D, lower panel, G392E, lane M, asterisk). The percentage of radiolabelled neuroserpin in the cell lysates and culture media for each variant was quantified by autoradiography (Fig. 3D, graph). The amount of secreted neuroserpin decreases with

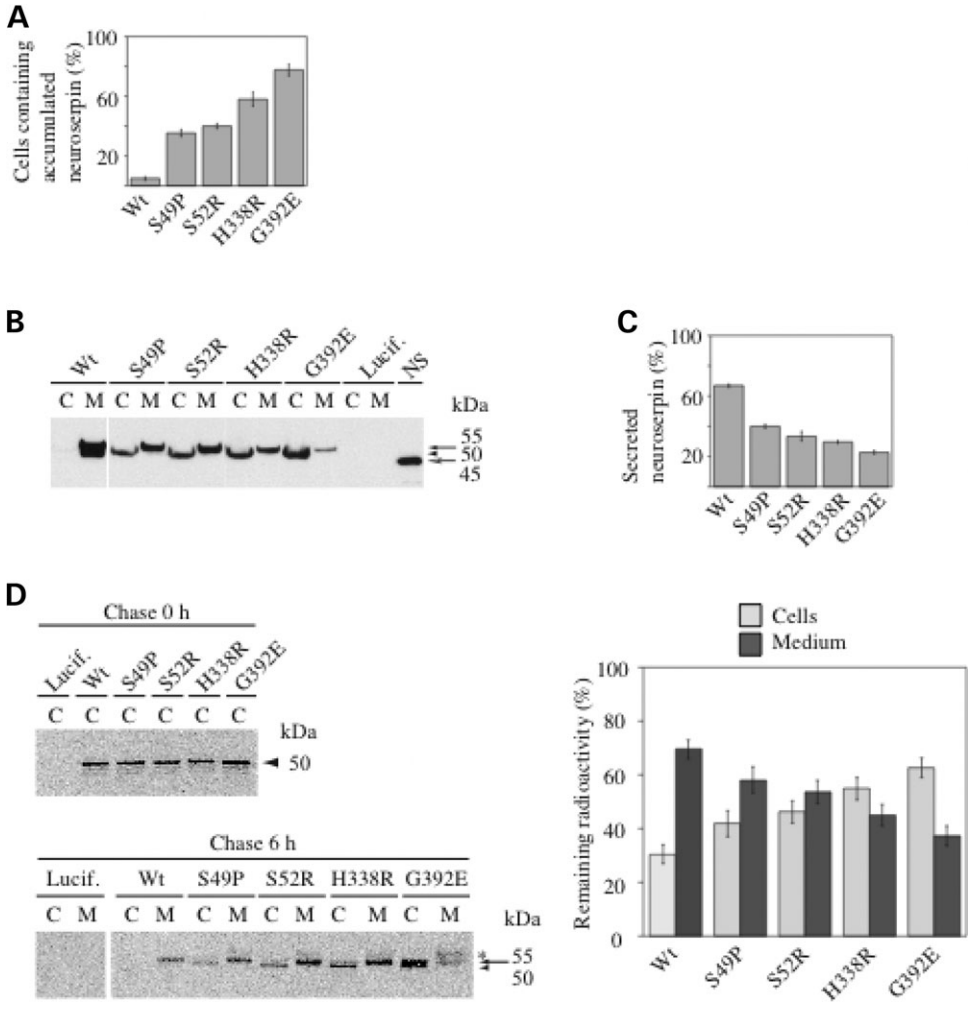

Figure 3. Increasing intracellular accumulation of mutant neuroserpin polymers correlates with increasing severity of FENIB. (**A**) Percentage of transfected COS-7 cells showing punctate neuroserpin accumulation 24 h after transfection. Neuroserpin accumulation was quantified by counting more than 100 transfected cells per experiment in three independent experiments for each neuroserpin variant. Each experiment was counted blind and cells were scored as containing punctate accumulation if there were at least 10 discrete protein 'spots' per cell. Percentages are averages $\pm$SEM, and the differences were statistically significant when analysed by one-way ANOVA ($P < 0.0001$) followed by a post-test for linear trend ($R^2 = 0.93$, $P < 0.0001$). (**B**) Cell lysates (C) and culture media (M) of COS-7 cells transfected with wild-type or each mutant neuroserpin or with a control plasmid expressing luciferase (Lucif.) were analysed 72 h after transfection by 8% w/v acrylamide SDS–PAGE and western-blot analysis with an anti-neuroserpin antibody. NS, control lane loaded with 20 ng of purified recombinant neuroserpin. Black arrow: fully glycosylated and secreted neuroserpin, 55 kDa; arrowhead: intracellular neuroserpin intermediate, 50 kDa; black and white arrow: non-glycosylated recombinant neuroserpin used as a control, 45 kDa. (**C**) The amount of total neuroserpin was determined by sandwich ELISA in cell lysates and culture media of COS-7 cells 72 h after transfection with wild-type or each mutant neuroserpin. The graph shows the proportion of neuroserpin that was present in the culture media. Values are averages $\pm$SEM from three independent repeats, and the differences were statistically significant when analysed by one-way ANOVA ($P < 0.0001$) followed by a post-test for linear trend ($R^2 = 0.82$, $P < 0.0001$). (**D**) Cells transfected with wild-type or each mutant neuroserpin were pulsed-labelled and chased for 6 h. Cells lysates (C) and culture media (M) were analysed by immunoprecipitation and 8% w/v SDS–PAGE. Arrow: fully glycosylated and secreted neuroserpin, 55 kDa; arrowhead: intracellular neuroserpin intermediate, 50 kDa; asterisk: a slower migrating second band in the culture medium of cells transfected with G392E neuroserpin. The graph shows the quantitation of the pulse-chase experiment using a phosphorimager. The amount of radioactivity in each sample is expressed as the percentage of the total radioactivity for each neuroserpin variant. Values are averages $\pm$SEM from five independent repeats, and the differences were statistically significant when analysed by one-way ANOVA ($P < 0.0001$) followed by a post-test for linear trend ($R^2 = 0.59$, $P < 0.0001$).

increasing propensity to form polymers: 70% of the wild-type neuroserpin was found in the culture medium and 59, 55, 45 and 38% of S49P, S52R, H338R and G392E neuroserpin, respectively (correlation coefficient $R^2 = 0.59$).

These results demonstrate that all known mutations in neuroserpin that cause polymerization lead to decreased secretion of the mutant protein, and that the defect in trafficking increases with increasing propensity to form polymers.

Polymer accumulation and decreased regulated secretion of mutant neuroserpin in PC12 cells

Neuroserpin is constitutively secreted in COS-7 cells. However, in glandular and neural tissues, neuroserpin is trafficked through the regulated secretory pathway, stored in dense core vesicles and secreted upon stimulation (22–24). We therefore developed stably transfected PC12 cell lines

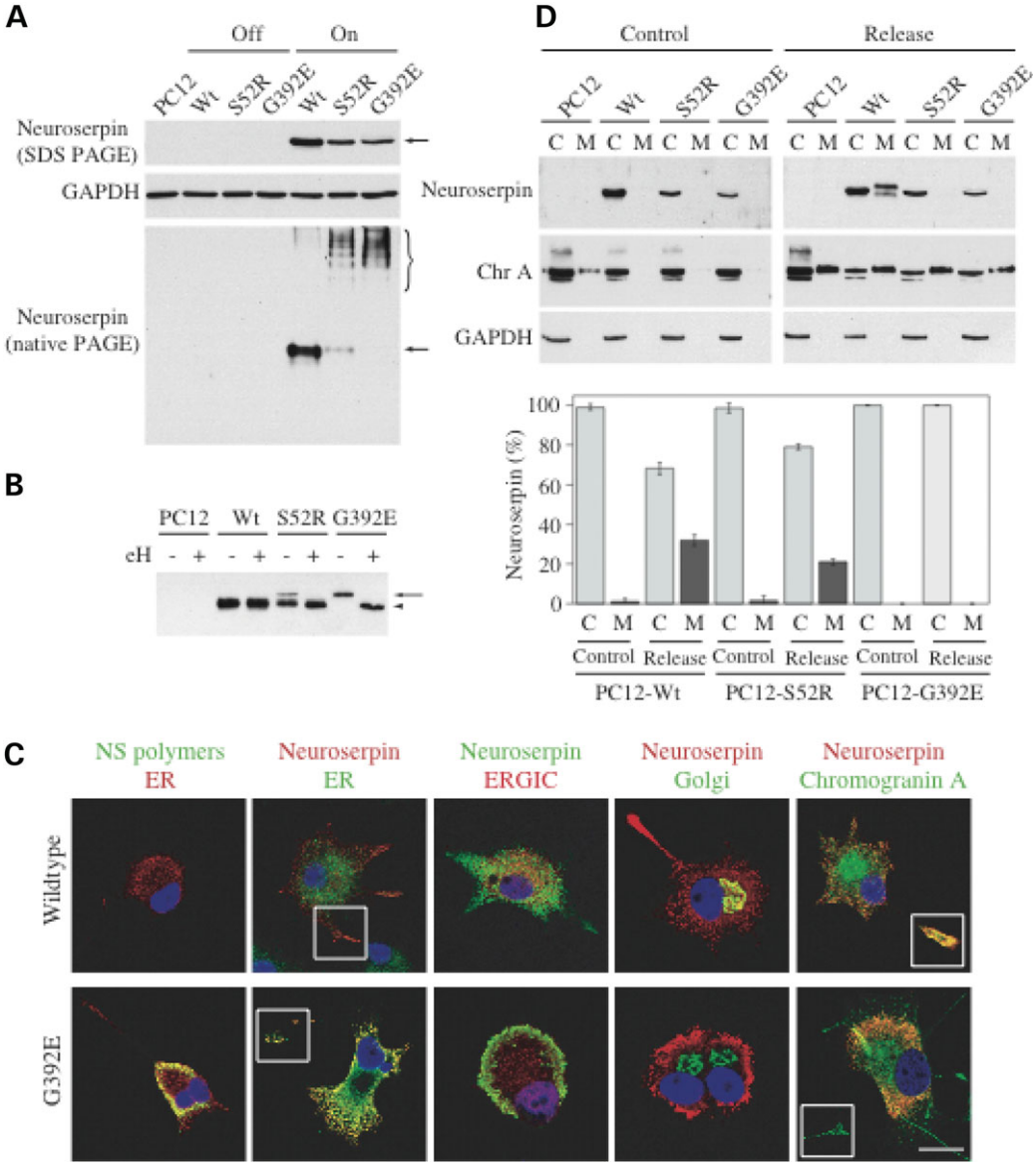

Figure 4. Trafficking of wild-type and mutant neuroserpin in stably transfected PC12 cell lines. (**A**) Lysates from PC12-Tet-On, PC12-Wt, PC12-S52R and PC12-G392E cells cultured with (*on*) or without (*off*) 10 μg/ml doxycycline to induce neuroserpin expression were analysed by SDS and non-denaturing PAGE followed by western-blot analysis with an anti-neuroserpin polyclonal antibody. The membrane from the SDS–PAGE was also analysed with an anti-GAPDH antibody as a loading control. (**B**) Neuroserpin from lysed PC12-Tet-On, PC12-Wt, PC12-S52R and PC12-G392E cells induced for 4 days was immunoprecipitated with the 1A10 anti-neuroserpin monoclonal antibody and treated (+) or not (−) with endoglycosidase H (eH) and analysed by SDS–PAGE and western blot analysis. S52R and G392E neuroserpin were sensitive to endoglycosidase H (arrow) whereas wild-type neuroserpin was resistant (arrowhead). (**C**) Immuno-co-localization of wild-type and G392E neuroserpin with resident proteins of the secretory pathway. PC12-wildtype and PC12-G392E cells were differentiated to a neuronal phenotype by plating in collagen and treating with NGF (150 ng/ml) for 7 days, and then induced to express neuroserpin with 10 μg/ml doxycycline for 3 days. Cells were co-stained with either a polyclonal anti-neuroserpin antibody or one of the anti-neuroserpin monoclonal antibodies (1A10 for total neuroserpin or 7C6 for neuroserpin polymers) and antibodies against calreticulin (ER), GM130 (Golgi), ERGIC-53/p58 (ERGIC) or chromogranin A (trafficked through the regulated secretory pathway). The colour corresponding to each antibody (red or green) is shown above the figure and only the merged images are presented. Yellow represents areas of overlapping red and green. The nucleus appears blue due to DNA staining with DAPI. Scale bar: 10 μm. (**D**) PC12-Wt, PC12-S52R and PC12-G392E cells were induced to express neuroserpin for 3 days with 10 μg/ml doxycycline and then incubated for 15 min with control or release buffer containing 5 or 55 mM KCl, respectively, to assess regulated secretion from dense core secretory granules. Neuroserpin was analysed in cell lysates and buffer solutions by SDS–PAGE and western blot and quantified by sandwich ELISA. The graph shows the averages for three independent experiments analysed by ELISA, expressed as percentages ± SEM. The amount of neuroserpin secreted from each cell line when treated with release buffer was statistically different when analysed by one-way ANOVA ($P = 0.0003$) followed by a post-test for linear trend ($R^2 = 0.93$, $P = 0.0001$).

that conditionally expressed wild-type neuroserpin (PC12-Wt) or mutants that cause moderate (S52R; PC12-S52R) and severe (G392E; PC12-G392E) forms of FENIB (Fig. 4A). Neuroserpin was detected by SDS–PAGE and western-blot analysis in lysates of the three cell lines following induction with doxycycline (Fig. 4A, top panel, lanes On). The steady-state level of neuroserpin was lower for cells expressing the mutant proteins. This must be due to increased

ER-associated degradation of S52R and G392E neuroserpin, as the three cell lines expressed similar levels of protein when assessed by the pulse-chase analysis (results not shown) and both mutant proteins accumulated within the cells upon treatment with the proteasomal inhibitors lactacystin and MG132 (data not shown). Non-denaturing PAGE and western-blot analysis of cell lysate from PC12-Wt cells showed a single band characteristic of monomeric wild-type neuroserpin (Fig. 4A, bottom panel, lane On/Wt, arrow), while PC12-S52R and PC12-G392E cell lysates showed high molecular mass ladders typical of polymers (Fig. 4A, bottom panel, lanes On/S52R and On/G392E, curly bracket). A weak monomeric band was also apparent in lysates from the PC12-S52R cells (Fig. 4A, bottom panel, lane On/S52R, arrow).

Neuroserpin from each of the cell lysates was characterized by immunoprecipitation with the 1A10 monoclonal antibody followed by endoglycosidase H digestion (Fig. 4B). The immunoprecipitate from PC12-Wt cells contained a single band that was unchanged following treatment with endoglycosidase H (Fig. 4B, Wt $-/+$), suggesting that at steady state the bulk of wild-type neuroserpin is present as mature protein in our PC12 cells. In contrast, neuroserpin immunoprecipitated from PC12-G392E cells ran as a single band of higher molecular mass that decreased in size following treatment with endoglycosidase H (Fig. 4B, G392E $-/+$). Thus, this protein had not trafficked to the Golgi apparatus. Lysates from PC12-S52R cells showed an intermediate situation with two neuroserpin bands in the immunoprecipitate, one similar in size to wild-type neuroserpin and a higher molecular mass band similar to that of G392E neuroserpin. This band also decreased in size after treatment with endoglycosidase H (Fig. 4B, S52$R-/+$).

Taken together, these results suggest that there are two different species of neuroserpin that can be differentiated after immunoprecipitation: monomeric wild-type and S52R neuroserpin, which are insensitive to endoglycosidase H digestion and run as single bands on non-denaturing PAGE, and polymers of S52R and G392E neuroserpin, which are endoglycosidase H sensitive and form high molecular mass ladders on non-denaturing PAGE.

The trafficking of neuroserpin was then assessed in PC12 cells that were differentiated into neurons by plating on collagen and treatment with nerve growth factor prior to the expression of neuroserpin. The distribution of total neuroserpin was characterized with an anti-neuroserpin polyclonal antibody while neuroserpin polymers were identified with the 7C6 monoclonal antibody. There was strong staining for wild-type neuroserpin in the periphery of the cells and the tips of neurites (Fig. 4C, wild type, outlined neurite tips) where it co-localized with chromogranin A (Fig. 4C, top, neuroserpin/chromogranin A, outlined neurite tip), a marker for dense core vesicles. This is in keeping with the storage of wild-type neuroserpin in dense core vesicles ready for regulated secretion. No polymers were detected with the 7C6 antibody in PC12-Wt cells (Fig. 4C, wild-type, NS polymers/ER). In contrast, G392E neuroserpin was found mainly in the cell body of PC12 cells where it formed punctate accumulations typical of mutant neuroserpin (Fig. 4C, G392E). These inclusions stained positive for both total neuroserpin and neuroserpin polymers (Fig. 4C, G392E, NS polymers/ER and Neuroserpin/ER). The analysis of PC12-S52R cells showed a mixture of the staining seen for wild-type and G392E neuroserpin (data not shown).

We concentrated on the wild-type and G392E neuroserpin cell lines for further characterization of neuroserpin trafficking by immunocytochemistry. Wild-type neuroserpin did not co-localize with calreticulin in the ER or ERGIC-53/p-58 in the ER Golgi intermediate compartment (ERGIC) and only some cells showed co-localization with GM130 in the Golgi compartment (Fig. 4C, wild type, neuroserpin/ER, neuroserpin/ERGIC, neuroserpin/Golgi). G392E neuroserpin co-localized with calreticulin within the ER even when the punctate inclusions were found within the neurites (Fig. 4C, G392E, neuroserpin polymers/ER and neuroserpin/ER, outlined neurite tip), but there was no co-localization with the ERGIC (Fig. 4C, G392E, neuroserpin/ERGIC) or Golgi markers (Fig. 4C, G392E, neuroserpin/Golgi). There was poor co-localization with chromogranin A and none within the neurites, indicating the absence of mutant neuroserpin in dense core secretory vesicles (Fig. 4C, G392E, neuroserpin/chromogranin A, outlined neurite tip).

In view of the co-localization of wild-type neuroserpin with chromogranin A, we assessed the regulated secretion of neuroserpin from each cell line upon stimulation with 55 mM KCl for 15 min. Cell lysates and media were analysed by SDS–PAGE and western-blot analysis and by sandwich ELISA. Treatment with K^+ resulted in the secretion of 30% of the wild-type neuroserpin, 20% of S52R neuroserpin (detectable only by ELISA) and no neuroserpin from cells expressing G392E neuroserpin (Fig. 4D western blot and graph, release). The same results were obtained with a second independent clone for each cell line (data not shown). The reduction in regulated secretion was specific for neuroserpin, since similar amounts of secreted chromogranin A were detected by western-blot for all the PC12 cell lines (Fig. 4D, chromogranin A/release).

Our results demonstrate that the stably transfected PC12 cell lines reproduce the physiological trafficking of neuroserpin through the regulated secretory pathway. In this model system, wild-type neuroserpin was synthesized, normally trafficked and stored as mature endoglycosidase H resistant protein in dense-core secretory vesicles at the tip of the neurites, from where it was released upon membrane depolarization. In contrast, mutant G392E neuroserpin was found in a pre-Golgi compartment and was not secreted upon stimulation. S52R neuroserpin showed an intermediate phenotype, with a fraction of the protein being trafficked and secreted and the remainder being retained in the ER. This demonstrates that increasing propensity to polymerization underlies increasing trafficking defects in correlation with human disease in the context of an expression system that is closer to human physiology.

The neuronal dysfunction underlying FENIB is caused by the accumulation of neuroserpin polymers

The expression of S52R and G392E neuroserpin in stably transfected PC12 cell lines did not result in demonstrable apoptosis as assessed by staining with antibodies against annexin V and active caspase-3, up to 12 days after induction

of expression (results not shown). The effect of long-term polymer accumulation was assessed at the organismal level by generating *Drosophila* strains that expressed either wild-type neuroserpin or each of the variants that cause FENIB, under the control of a neuronal promoter. The expression of wild-type neuroserpin was toxic to the flies, therefore the key P1 and P1′ amino acids of neuroserpin, which are located in the reactive centre loop and form the pseudosubstrate for the target proteinase, were changed from Met-Arg to Pro–Pro. This mutation rendered recombinant neuroserpin purified from *E. coli* inactive as an inhibitor of tPA (29), but had no effect on the rate of polymerization (data not shown). The expression of wild-type neuroserpin with the P1–P1′ Pro–Pro substitution was no longer toxic to the fly (29). We therefore expressed all neuroserpin variants with Pro–Pro in the P1–P1′ positions in the nervous system of the fly under the control of the $elav^{c155}$ −Gal4 driver. At least five independent transgenic lines were generated for each genotype. Neuroserpin was detectable in fly homogenates in all lines by sandwich ELISA, although the signal was lower in flies expressing the wild-type protein probably as a result of efficient clearance (Fig. 5A). We selected one line for each genotype that was representative of the level of accumulation of neuroserpin. These lines were then characterized in more detail.

The distribution of neuroserpin in fly brain sections was assessed by immunohistochemistry with the monoclonal antibody 1A10. There was intracellular accumulation of each of the mutant proteins in the cell bodies of heterogeneously distributed cortical neurons. This was despite $elav^{c155}$ −Gal4 driving ubiquitous neuronal expression (Fig. 5B S49P, S52R, H338R and G392R panels, and enlarged details for S52R and G392E). Cells containing accumulated neuroserpin were most abundant in flies expressing the H338R and G392E mutants of neuroserpin that cause severe FENIB. The low levels of wild-type neuroserpin already observed by ELISA precluded its localization by immunohistochemistry (Fig. 5B, Wt).

The anti-polymer monoclonal antibody 7C6 does not stain paraffin sections; we were therefore unable to correlate the accumulation of mutant neuroserpin with the presence of polymers by immunohistochemistry. We were, however, able to detect and quantify polymerized neuroserpin in brain homogenates by sandwich ELISA using the 7C6 monoclonal antibody (Fig. 5C). There was marked accumulation of neuroserpin polymers in flies expressing mutant neuroserpin, particularly the highly polymerogenic H338R and G392E mutants. This correlated well with the results obtained by immunohistochemistry and provides evidence that the signal detected by immunohistochemistry corresponds to the accumulation of polymers. We were unable to detect polymers in the brains of flies expressing wild-type protein (Fig. 5C).

Having confirmed that neuroserpin polymer accumulation only occurs in flies expressing disease-causing variants, we then examined the effects of mutant neuroserpin expression on survival of flies and their neurological function. There was no difference in median survival of flies expressing wild type (39 days, $n = 60$), S49P (41 days, $n = 60$), S52R (39 days, $n = 60$), H338R (39 days, $n = 60$) or G392E (45 days, $n = 60$) neuroserpin when compared to control flies ($elav^{c155} \times w^{1118}$, 39 days, $n = 60$) (Fig. 5D). Locomotor function was normal in flies expressing wild-type and mutant neuroserpin at eclosion (emergence of the adult from the pupa) but deteriorated rapidly in flies expressing mutant neuroserpin. By day 30 after eclosion, there were clear deficits in climbing that correlated with the level of accumulation of neuroserpin polymers (correlation coefficient 0.84, $P < 0.05$; Fig. 5E). Additionally, the expression of neuroserpin in the eye with the GMR-Gal4 driver caused a rough eye phenotype for all the mutants that form polymers but not in flies expressing the wild-type protein (data not shown). These data provide a direct link between the accumulation of neuroserpin polymers over time and neurological dysfunction.

DISCUSSION

The neurodegenerative disorder familial encephalopathy with neuroserpin inclusion bodies (FENIB) results from point mutations in the neuroserpin gene. We have investigated how four different mutations in neuroserpin cause dementia by assessing the mechanism of disease at the cellular and organismal level. We show that all four point mutations lead to polymerization of neuroserpin, and that this in turn slows the trafficking of the mutant protein from the ER, thereby causing polymer accumulation in the ER lumen. The parallel analysis of different mutations has allowed us to establish that the severity of the trafficking defect correlates directly with the severity of the disease phenotype. Finally, we show that the long-term accumulation of neuroserpin polymers within neurons causes a locomotor deficit in flies, supporting the hypothesis that serpin polymers are the toxic species in FENIB.

Our previous work has characterized the trafficking of S49P and S52R mutants of neuroserpin that underlie mild/moderate forms of FENIB (27). We now demonstrate that H338R and G392E neuroserpin also form polymers that are retained as intracellular inclusions when transiently expressed in COS-7 cells (Fig. 1). When all four mutants were analysed in parallel, the degree of retention was directly proportional to the length of the polymers and the severity of the clinical phenotype caused by each mutation. Thus, the mutant of neuroserpin that causes the most severe clinical phenotype, G392E neuroserpin, formed the longest chain polymers and showed the greatest degree of intracellular retention followed by H338R, S52R and S49P neuroserpin (Figs 1C and 3). No polymers were detected following the expression of wild-type neuroserpin (Figs 1C and 2C). These data provide strong experimental support for molecular models predicting the propensity of neuroserpin mutants to form polymers *in vivo*. We confirmed the presence of polymers using a novel conformer specific anti-neuroserpin polymer monoclonal antibody. This antibody and digestion with endoglycosidase H, localized the polymerized neuroserpin to the ER, in keeping with previous observations from patients with FENIB (12) and mice overexpressing mutant neuroserpin (28), and with findings from COS-7 cells transiently transfected with S49P and S52R neuroserpin (27).

Transient transfection experiments in COS-7 cells do not provide information on the effects of long-term expression

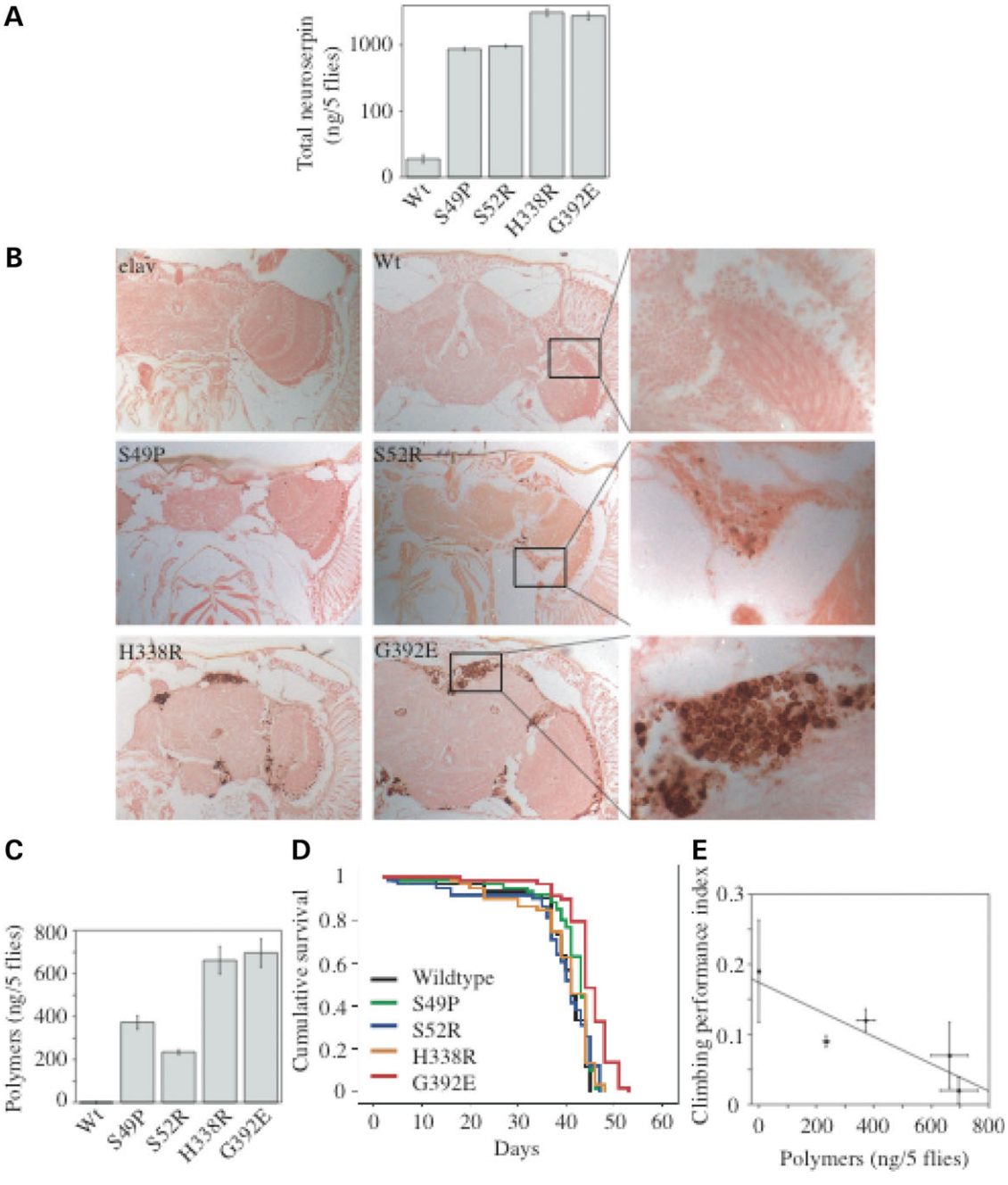

Figure 5. Polymers of mutant neuroserpin accumulate in the brain of transgenic flies and cause a locomotor phenotype. (**A**) Levels of total neuroserpin were determined in transgenic fly homogenates (see Materials and Methods) by sandwich ELISA. (**B**) Immunohistochemical detection of neuroserpin with the 1A10 monoclonal antibody in the brains of flies expressing the *elav* promotor (elav), wild-type (Wt), S49P (S49P), S52R (S52R), H338R (H338R) or G392E (G392E) neuroserpin at day 25 after eclosion. Intracellular accumulation of mutant neuroserpin (brown staining) was located within cortical neuronal cell bodies, adjacent to the mushroom bodies and lobula. Left and middle panels were taken with a 20× objective, enlarged details in right panels were obtained with a 100× oil immersion objective. (**C**) Levels of polymerized neuroserpin were determined in transgenic fly homogenates (see Materials and Methods) by sandwich ELISA with the 7C6 monoclonal antibody. (**D**) Cumulative survival plots for a hundred flies of each representative line chosen for each neuroserpin genotype. (**E**) Transgenic flies expressing all five variants of neuroserpin were subjected to climbing assays (see Materials and Methods) to assess their locomotor performance and the results were plotted against the levels of neuroserpin polymers detected by ELISA in (**C**). A negative correlation was found with an $R^2 = 0.84$ that was statistically significant at $P < 0.05$.

of neuroserpin or how the mutants are handled by the regulated secretory pathway (22–24). We addressed these questions by generating stable transfected PC12 lines that conditionally express wild-type, S52R and G392E neuroserpin. These mutants were selected as they cause moderate and severe forms of FENIB, respectively. The induction of S52R and G392E neuroserpin resulted in the formation of polymers that accumulated within undifferentiated PC12 cells (Fig. 4A).

The mutants were also handled differently from the wild-type protein when the PC12 cells were differentiated into neurons by treatment with NGF. Wild-type neuroserpin co-localized with chromogranin A at the tips of neurites, most likely in the dense-core secretory vesicles (Fig. 4C). It was present as a mature protein (insensitive to digestion with endoglycosidase H) that was released upon stimulation with high concentrations of extracellular potassium (Fig. 4B and D). Thus, wild-type neuroserpin showed the normal behaviour of a protein processed through the regulated secretory pathway. In contrast, G392E neuroserpin was retained within the ER as an endoglycosidase H sensitive protein that formed polymers when assessed by non-denaturing PAGE and by immunocytochemistry with our anti-neuroserpin polymer monoclonal antibody. This would explain the lack of regulated secretion of this mutant protein after membrane depolarization with potassium. It is striking that the S52R mutant, which causes moderately severe FENIB, showed characteristics that are intermediate between wild-type and G392E neuroserpin. A proportion of S52R neuroserpin reached the dense-core secretory vesicles for secretion, whereas a proportion formed polymers that accumulated within the ER. These findings underscore the correlation between the polymerization and trafficking defects of the different mutations of neuroserpin and the severity of the clinical phenotype of FENIB.

A similar correlation between polymer formation and intracellular retention has been described for point mutations in the serpin α_1-antitrypsin. The Z mutation (Glu342Lys) causes α_1-antitrypsin to form polymers within hepatocytes more rapidly than the milder S (Glu264Val) or I (Arg39Cys) variants (30). This is associated with a greater retention of intracellular Z α_1-antitrypsin, which in turn is associated with more inclusions, a greater risk of liver disease and more severe plasma deficiency. This genotype–phenotype correlation was established by correlating the rate of α_1--antitrypsin polymerization *in vitro* with the clinical manifestations caused by each mutant of α_1-antitrypsin (8). Our current study is the first to provide a direct correlation between the intracellular formation of serpin polymers and the severity of a clinical phenotype of a serpinopathy.

Our findings raise the important and unresolved question of whether the retention of intracellular polymers is intrinsically toxic. This was assessed in a whole organism by expressing wild-type neuroserpin and the mutants that cause FENIB in the neurones of flies. In all cases, the protease inhibitory activity of neuroserpin was removed by expressing the protein with Pro–Pro residues in the P1–P1′ positions of the reactive site loop. P1–P1′ Pro–Pro wild-type neuroserpin was not retained within neurones and had no effect on the longevity of the flies or their locomotor performance (Fig. 5). In contrast, the mutant forms of neuroserpin formed polymers that accumulated heterogeneously within the cell bodies of cortical neurones (Fig. 5). This was despite the ubiquitous expression of neuroserpin in all neurones of the brain. The distribution of neuroserpin inclusions in flies resembles the distribution in the brains of patients (12,13) and in mouse models (28) of FENIB. The degree of protein accumulation was directly proportional to the severity of the disease phenotype caused by each mutation and mirrored the findings from both transiently transfected COS-7 cells and the conditional expression of neuroserpin in PC12 cells. The expression of the different forms of neuroserpin had no effect on the longevity of the flies, but there was a progressive reduction in fly locomotor function that correlated with the quantity of neuroserpin polymers in the brain (Fig. 5). These data provide strong evidence that the accumulation of polymers within neurones is neurotoxic *in vivo*. Moreover, the level of toxicity is directly proportional to the quantity of intracellular polymers. An alternative explanation of our results is that folding intermediates of mutant neuroserpin cause toxicity prior to polymerization. However, the expression of the Z mutant of α_1-antitrypsin does not activate the unfolded protein response (31–33), which indicates that polymerogenic serpins do not cause ER stress through the accumulation of mis-folded intermediates. It has recently been proposed that Z α_1-antitrypsin polymers are sequestered within ER derived inclusion bodies, protecting the cells from toxicity and allowing normal ER function (34). Although this seems probable in the short term and agrees with the lack of a strong toxicity phenotype in our cell and fly models of disease, the locomotor phenotype that we observe in flies that express mutant neuroserpin supports the toxicity of long-term accumulation of polymers within cells. Previous work has shown that the accumulation of the polymerogenic Z mutant of α_1-antitrypsin in cell models and in the livers of transgenic mice causes the activation of NF-kappa B (nuclear factor kappa B) (31,32), a hallmark of the ER overload response (35,36). The toxicity of neuroserpin polymers may also be mediated through this pathway.

In summary, mutants of neuroserpin form polymers within the ER at a level that is directly proportional to the severity of the clinical phenotype caused by these mutations. The degree of intracellular accumulation of polymers correlates with the severity of the progressive decline in locomotor function in *Drosophila* models of FENIB. Taken together these data allow us to conclude that neuroserpin polymers have an intrinsic toxicity that directly contributes to the clinical phenotype of FENIB.

MATERIALS AND METHODS

Reagents and antibodies

Unless stated otherwise, reagents, buffers, culture media and serum for cell cultures were from Sigma-Aldrich Co. (Dorset, UK). Custom made rabbit polyclonal anti-neuroserpin antibody (18), rabbit polyclonal anti-GAPDH, donkey polyclonal anti-rabbit IgG (Texas Red), anti-goat IgG (FITC) and anti-mouse IgG (FITC) antibodies were from Abcam (Cambridge, UK). Goat polyclonal anti-rabbit IgG (HRP), rabbit polyclonal anti-mouse IgG (HRP), goat polyclonal anti-mouse IgG, mouse peroxidase anti-peroxidase complex (mouse PAP) and rabbit polyclonal anti-ERGIC-53/p58 antibodies were from Sigma-Aldrich Co. Goat polyclonal anti-calreticulin and anti-chromogranin A antibodies were from Santa Cruz Biotechnology (through Autogen Bioclear, Mile Elm Calne, UK). Mouse monoclonal anti-GM130 antibody was from BD Biosciences Pharmigen (Oxford, UK).

Construction of neuroserpin expression plasmids

The plasmids expressing human wild-type, S49P and S52R neuroserpin are described in (27). H338R and G392E neuroserpin were generated from wild-type neuroserpin by site-directed mutagenesis with the QuikChange Site-Directed Mutagenesis kit (Stratagen, La Jolla, CA, USA). Wild-type, S52R and G392E neuroserpin were subcloned into the pTRE-Tight vector (BD Biosciences, Oxford, UK) for the generation of the stable PC12 Tet-On neuroserpin cell lines.

Cos-7 cell cultures, DNA transfections and analysis

COS-7 cells were maintained and transfected with DNA as described previously (27). SDS and non-denaturing PAGE followed by western-blot analysis, metabolic labelling and immunoprecipitation and immunocytochemistry for confocal microscopy were performed as described previously (27).

Generation and characterization of stable Tet-On PC12 cells lines expressing neuroserpin

The PC12 Tet-On cell line was purchased from BD Biosciences. Stable PC12-neuroserpin cell lines were generated following the instructions from BD Biosciences and screened for neuroserpin expression by ELISA (see below). The cells were cultured in DMEM supplemented with 10% v/v heat inactivated horse serum, 5% v/v Tet Approved FBS (BD Biosciences), 1% v/v HEPES buffer, 0.2 U/ml bovine insulin, 200 μg/ml Geneticin and 100 μg/ml Hygromycin B (both selective antibiotics from Invitrogen, Paisley, UK), at 37°C and 5% v/v CO_2 in a humidified incubator. Neuroserpin expression was typically induced for 4 days with 10 μg/ml doxycycline. SDS and non-denaturing PAGE followed by western-blot analysis and immunocytochemistry for confocal microscopy were performed as described previously (27). Rabbit anti-neuroserpin polyclonal antibody was diluted at 1:750, anti-neuroserpin monoclonal antibodies were used at 1 μg/ml, anti-calreticulin and anti-GM130 were used at 1 μg/ml, anti-chromogranin A was used at 4 μg/ml, anti-ERGIC-53/p58 was used at 5 μg/ml and donkey secondary anti-rabbit IgG (Texas Red), anti-goat IgG (FITC) and anti-mouse IgG (FITC) antibodies were used at 1.3 ng/μl.

To assess the regulated secretion, cells were treated with 1 ml/well of control or release buffer (control: 5 mM KCl, 125 mM NaCl, 1.2 mM $MgCl_2$, 1 μM $ZnCl_2$, 4.5 g/l w/v D-glucose, 25 mM hepes, 5.2 mM $CaCl_2$; release: same as control except 55 mM KCl and 70 mM NaCl) for 15 min at 37°C. The supernatants were cleared by spinning at 500 g for 10 min and the cell lysates were prepared as described previously (27).

PC12 cells were differentiated into neurones by plating onto glass coverslips pre-treated with 0.1 mg/ml poly-L-lysine and 0.1 mg/ml rat tail collagen I and culturing in DMEM supplemented with 1% v/v heat inactivated horse serum, non-essential amino acids, HEPES buffer, 0.2 U/ml bovine insulin, 200 μg/ml Geneticin100 μg/ml Hygromycin B and 150 ng/ml nerve growth factor for 7 days.

Production of the anti-neuroserpin monoclonal antibodies

Mice immunizations and spleen isolation were carried out by Harlan Sera-Lab (Belton, Leicestershire, UK). Three mice were immunized with recombinant S49P neuroserpin polymers (five doses of 10, 20 and 40 μg, respectively) and one was immunized with S49P neuroserpin polymers extracted from neuroserpin inclusions isolated from patients with FENIB (26) (five doses of 8 μg). The production of hybridoma cell lines was carried out as described previously (37,38). The hybridoma clones were screened by antigen-mediated ELISA using purified recombinant wild-type neuroserpin or S49P neuroserpin polymers as the antigen. Selected clones were sub-cloned by limited dilution and expanded as cell lines.

Sandwich ELISA

Unless stated otherwise, all steps were carried out at room temperature and using 50 μl/well. Plates (Corning Inc., Costar 3590) were coated overnight at 4°C with antigen-purified rabbit polyclonal anti-neuroserpin antibody at 2 μg/ml in 0.2 M $Na_2CO_3/NaHCO_3$ pH 9.4. Next, wells were washed with 0.9% w/v NaCl, 0.05% v/v Tween20 and blocked for 2 h with 300 μl/well of blocking buffer (PBS, 0.25% w/v BSA, 0.05% v/v Tween20, 0.025% w/v Na azide). Standards (recombinant purified wild-type or polymerized mutant neuroserpin) and unknown samples (cell lysates prepared as for western-blot, culture medium supernatants or fly extracts, see below) were diluted in blocking buffer and incubated for 2 h. After washing, the wells were incubated with either a pool of monoclonal antibodies (1A10, 10B8 and 10G12, each 333 ng/ml) or with an individual monoclonal antibody (1 μg/ml) diluted in blocking buffer for 2 h. Bound monoclonal antibodies were detected with rabbit anti-mouse HRP antibody (1:20000 in blocking buffer without Na azide) for 1 h. After developing for 10 min with TMB substrate solution (Sigma-Aldrich Co, Dorset, UK) and stopping the reaction with 1 M H_2SO_4, HRP activity was measured in a plate reader (Molecular Devices, Thermo-max microplate reader) at 450 nm.

Fly culture and generation of transgenic flies

All stocks were in a w^{1118} background, cultured on standard fly food with dried yeast and maintained at 29°C. Transgene expression was driven with the *elav-Gal4* pan-neuronal driver or the GMR-Gal4 retinal driver, as indicated. Transgenic fly lines containing wild-type, S49P, S52R, H338R and G392E neuroserpin transgenes were generated with the human secretion signal peptide in the *Gal4*-responsive pUAST expression vector. Relative expression levels were determined with reverse-transcriptase quantitative PCR (RT–qPCR) and transgene expression was found to vary by less than 8-fold between lines. Representative lines, chosen according to their level of neuroserpin accumulation, were used in all experiments.

Preparation of fly samples for ELISA

Female flies were collected 35 days after eclosion. Three aliquots of five whole flies were homogenized in 100 μl of 150 mM NaCl, 50 mM Tris pH 7.5, 5 mM EDTA and protease inhibitor cocktail tablets (Roche) using mortar and pestle (Fisher Scientific, Loughborough, UK). After clearing by centrifugation (16000 g for 15 min), the supernatant was retrieved avoiding any lipid droplets.

Immunohistochemistry in fly sections

Heads were dissected from female flies 25 days after eclosion. Paraffin sections were deparaffinated, rehydrated and treated for 10 min in the dark with 10% v/v methanol, 3% v/v H_2O_2 in PBS to inactivate endogenous peroxidase activity. Sections were then incubated with 1A10 monoclonal antibody at 25 μg/ml in blocking reagent (PBS, 10% w/v BSA, 0.1% v/v Triton X-100, 0.1% w/v Na azide) overnight at room temperature. After three washes in PBS, sections were incubated with anti-mouse IgG at 80 μg/ml for 45 min and mouse PAP complex at 1:200 for 30 min (in Na azide free-blocking reagent), with three washes in PBS after each incubation step. HRP activity was developed with SIGMAFAST-DAB tablets (Sigma-Aldrich Co., Dorset, UK) and sections were subsequently dehydrated and mounted with DePex (VWR International, Lutterworth, UK). Pictures were obtained in a Zeiss AxioSkope2 microscope using AxioVision software.

Climbing assays

Climbing assays were performed as previously described (39). Briefly, female flies were transferred to 25 ml pipettes in groups of 15. Flies were tapped down to the bottom of the tube and 30 s later the number of flies at the top and at the bottom were counted. Each tube was tested three times. Two or three cohorts of 15 flies were tested for each genotype. The performance index (PI) for each tube of flies was calculated as $PI = 0.5 \times ((\text{Total flies} + \text{flies at top} - \text{flies at bottom})/\text{total flies})$ to give a score between 0 and 1.

ACKNOWLEDGEMENTS

We are grateful to Dr Richard Davis, Department of Pathology, Upstate Medical University, Syracuse, New York, USA for providing the Collins bodies used for the extraction of human S49P neuroserpin polymers. We also thank Matthew Gratian and Mark Bowen, Cambridge Institute for Medical Research, for technical support and all members of the Lomas lab and G. Lupo for helpful discussions. Funding to pay the Open Access publication charges for this article was provided by The Wellcome Trust.

Conflict of Interest statement. The authors declare that they have no conflicts of interest.

FUNDING

This work was supported by the Medical Research Council (UK), the Wellcome Trust and Papworth NHS Trust. K.R. was a Wellcome Trust Senior Fellow (Grant 042216). J.P. was supported by the Ministerio de Educación y Ciencia (Grant PR2007-0018 and BFU 2006 11754) and the Junta de Andalucía (Grant P07 CVI 03079) (Spain).

REFERENCES

1. Carrell, R.W. and Lomas, D.A. (1997) Conformational diseases. *Lancet*, **350**, 134–138.
2. Lomas, D.A. and Mahadeva, R. (2002) Alpha-1-antitrypsin polymerisation and the serpinopathies: pathobiology and prospects for therapy. *J. Clin. Invest.*, **110**, 1585–1590.
3. Kaiserman, D., Whisstock, J.C. and Bird, P.I. (2006) Mechanisms of serpin dysfunction in disease. *Expert Rev. Mol. Med.*, **8**, 1–19.
4. Huntington, J.A., Pannu, N.S., Hazes, B., Read, R., Lomas, D.A. and Carrell, R.W. (1999) A 2.6Å structure of a serpin polymer and implications for conformational disease. *J. Mol. Biol.*, **293**, 449–455.
5. Dunstone, M.A., Dai, W., Whisstock, J.C., Rossjohn, J., Pike, R.N., Feil, S.C., Le Bonniec, B.F., Parker, M.W. and Bottomley, S.P. (2000) Cleaved antitrypsin polymers at atomic resolution. *Protein Sci.*, **9**, 417–420.
6. Lomas, D.A., Evans, D.L., Finch, J.T. and Carrell, R.W. (1992) The mechanism of Z α_1-antitrypsin accumulation in the liver. *Nature*, **357**, 605–607.
7. Elliott, P.R., Lomas, D.A., Carrell, R.W. and Abrahams, P. (1996) Inhibitory conformation of the reactive loop of α_1-antitrypsin. *Nat. Struct. Biol.*, **3**, 676–681.
8. Dafforn, T.R., Mahadeva, R., Elliott, P.R., Sivasothy, P. and Lomas, D.A. (1999) A kinetic description of the polymerisation of α_1-antitrypsin. *J. Biol. Chem.*, **274**, 9548–9555.
9. Sivasothy, P., Dafforn, T.R., Gettins, P.G.W. and Lomas, D.A. (2000) Pathogenic α_1-antitrypsin polymers are formed by reactive loop-β-sheet A linkage. *J. Biol. Chem.*, **275**, 33663–33668.
10. Lomas, D.A. and Carrell, R.W. (2002) Serpinopathies and the conformational dementias. *Nat. Rev. Genet.*, **3**, 759–768.
11. Perlmutter, D.H. (2002) Liver injury in α_1-antitrypsin deficiency: an aggregated protein induces mitochondrial injury. *J. Clin. Invest.*, **110**, 1579–1583.
12. Davis, R.L., Shrimpton, A.E., Holohan, P.D., Bradshaw, C., Feiglin, D., Sonderegger, P., Kinter, J., Becker, L.M., Lacbawan, F., Krasnewich, D. *et al.* (1999) Familial dementia caused by polymerisation of mutant neuroserpin. *Nature*, **401**, 376–379.
13. Davis, R.L., Holohan, P.D., Shrimpton, A.E., Tatum, A., Daucher, J., Collins, G.H., Todd, R., Bradshaw, C., Kent, P., Feiglin, D. *et al.* (1999) Familial encephalopathy with neuroserpin inclusion bodies (FENIB). *Am. J. Pathol.*, **155**, 1901–1913.
14. Davis, R.L., Shrimpton, A.E., Carrell, R.W., Lomas, D.A., Gerhard, L., Baumann, B., Lawrence, D.A., Yepes, M., Kim, T.S., Ghetti, B. *et al.* (2002) Association between conformational mutations in neuroserpin and onset and severity of dementia. *Lancet*, **359**, 2242–2247.
15. Osterwalder, T., Contartese, J., Stoeckli, E.T., Kuhn, T.B. and Sonderegger, P. (1996) Neuroserpin, an axonally secreted serine protease inhibitor. *EMBO J.*, **15**, 2944–2953.
16. Osterwalder, T., Cinelli, P., Baici, A., Pennella, A., Krueger, S.R., Schrimpf, S.P., Meins, M. and Sonderegger, P. (1998) The axonally secreted serine proteinase inhibitor, neuroserpin, inhibits plasminogen activators and plasmin but not thrombin. *J. Biol. Chem.*, **237**, 2312–2321.
17. Hastings, G.A., Coleman, T.A., Haudenschild, C.C., Stefansson, S., Smith, E.P., Barthlow, R., Cherry, S., Sandkvist, M. and Lawrence, D.A. (1997) Neuroserpin, a brain-associated inhibitor of tissue plasminogen activator is localized primarily in neurones. *J. Biol. Chem.*, **272**, 33062–33067.
18. Belorgey, D., Crowther, D.C., Mahadeva, R. and Lomas, D.A. (2002) Mutant neuroserpin (Ser49Pro) that causes the familial dementia FENIB is a poor proteinase inhibitor and readily forms polymers *in vitro*. *J. Biol. Chem.*, **277**, 17367–17373.
19. Barker-Carlson, K., Lawrence, D.A. and Schwartz, B.S. (2002) Acyl-enzyme complexes between tissue type plasminogen activator and neuroserpin are short lived *in vitro*. *J. Biol. Chem.*, **277**, 46852–46857.
20. Miranda, E. and Lomas, D.A. (2006) Neuroserpin: a serpin to think about. *Cell. Mol. Life Sci.*, **63**, 709–722.

21. Galliciotti, G. and Sonderegger, P. (2006) Neuroserpin. *Front. Biosci.*, **11**, 33–45.
22. Hill, R.M., Parmar, P.K., Coates, L.C., Mezey, E., Pearson, J.F. and Birch, N.P. (2000) Neuroserpin is expressed in the pituitary and adrenal glands and induces the extension of neurite-like processes in AtT-20 cells. *Biochem. J.*, **345**, 595–601.
23. Parmar, P.K., Coates, L.C., Pearson, J.F., Hill, R.M. and Birch, N.P. (2002) Neuroserpin regulates neurite outgrowth in nerve growth factor treated PC12 cells. *J. Neurochem.*, **82**, 1406–1415.
24. Ishigami, S., Sandkvist, M., Tsui, F., Moore, E., Coleman, T.A. and Lawrence, D.A. (2007) Identification of a novel targeting sequence for regulated secretion in the serine protease inhibitor neuroserpin. *Biochem. J.*, **402**, 25–34.
25. Belorgey, D., Sharp, L.K., Crowther, D.C., Onda, M., Johansson, J. and Lomas, D.A. (2004) Neuroserpin Portland (Ser52Arg) is trapped as an inactive intermediate that rapidly forms polymers: implications for the epilepsy seen in the dementia FENIB. *Eur. J. Biochem.*, **271**, 3360–3367.
26. Onda, M., Belorgey, D., Sharp, L.K. and Lomas, D.A. (2005) Latent Ser49Pro neuroserpin forms polymers in the dementia familial encephalopathy with neuroserpin inclusion bodies. *J. Biol. Chem.*, **I280**, 13735–13741.
27. Miranda, E., Romisch, K. and Lomas, D.A. (2004) Mutants of neuroserpin that cause dementia accumulate as polymers within the endoplasmic reticulum. *J. Biol. Chem.*, **279**, 28283–28291.
28. Galliciotti, G., Glatzel, M., Kinter, J., Kozlov, S.V., Cinelli, P., Rulicke, T. and Sonderegger, P. (2007) Accumulation of mutant neuroserpin precedes development of clinical symptoms in familial encephalopathy with neuroserpin inclusion bodies. *Am. J. Pathol.*, **170**, 1305–1313.
29. Kinghorn, K.J., Crowther, D.C., Sharp, L.K., Nerelius, C., Davis, R.L., Chang, H.T., Green, C., Gubb, D.C., Johansson, J. and Lomas, D.A. (2006) Neuroserpin binds Abeta and is a neuroprotective component of amyloid plaques in Alzheimer disease. *J. Biol. Chem.*, **281**, 29268–29277.
30. Lomas, D.A. (2005) Molecular mousetraps, alpha1-antitrypsin deficiency and the serpinopathies. *Clin. Med.*, **5**, 249–257.
31. Lawless, M.W., Greene, C.M., Mulgrew, A., Taggart, C.C., O'Neill, S.J. and McElvaney, N.G. (2004) Activation of endoplasmic reticulum-specific stress responses associated with the conformational disease Z alpha 1-antitrypsin deficiency. *J. Immunol.*, **172**, 5722–5726.
32. Hidvegi, T., Schmidt, B.Z., Hale, P. and Perlmutter, D.H. (2005) Accumulation of mutant alpha1-antitrypsin Z in the endoplasmic reticulum activates caspases-4 and -12, NFkappaB, and BAP31 but not the unfolded protein response. *J. Biol. Chem.*, **280**, 39002–39015.
33. Graham, K.S., Le, A. and Sifers, R.N. (1990) Accumulation of the insoluble PiZ variant of human α_1-antitrypsin within the hepatic endoplasmic reticulum does not elevate the steady-state level of grp78/BiP. *J. Biol. Chem.*, **265**, 20463–20468.
34. Granell, S., Baldini, G., Mohammad, S., Nicolin, V., Narducci, P. and Storrie, B. (2008) Sequestration of mutated {alpha}1-antitrypsin into inclusion bodies is a cell protective mechanism to maintain endoplasmic reticulum function. *Mol. Biol. Cell.*, **19**, 572–586.
35. Pahl, H.L. and Baeuerle, P.A. (1997) The ER-overload response: activation of NF-kappa B. *Trends Biochem. Sci.*, **22**, 63–67.
36. Pahl, H.L. and Baeuerle, P.A. (1995) A novel signal transduction pathway from the endoplasmic reticulum to the nucleus is mediated by transcription factor NF-kappa B. *EMBO J.*, **14**, 2580–2588.
37. Perez, J., Peruzzo, B., Estivill-Torrus, G., Cifuentes, M., Schoebitz, K., Rodriguez, E. and Fernandez-Llebrez, P. (1995) Light- and electron-microscopic immunocytochemical investigation of the subcommissural organ using a set of monoclonal antibodies against the bovine Reissner's fiber. *Histochem. Cell Biol.*, **104**, 221–232.
38. Perez, J., Garrido, O., Cifuentes, M., Alonso, F.J., Estivill-Torrus, G., Eller, G., Nualart, F., Lopez-Avalos, M.D., Fernandez-Llebrez, P. and Rodriguez, E.M. (1996) Bovine Reissner's fiber (RF) and the central canal of the spinal cord: an immunocytochemical study using a set of monoclonal antibodies against the RF-glycoproteins. *Cell. Tissue Res.*, **286**, 33–42.
39. Crowther, D.C., Kinghorn, K.J., Miranda, E., Page, R., Curry, J.A., Duthie, F.A., Gubb, D.C. and Lomas, D.A. (2005) Intraneuronal Abeta, non-amyloid aggregates and neurodegeneration in a Drosophila model of Alzheimer's disease. *Neuroscience*, **132**, 123–135.